Clays and Clay Minerals, Vol. 69, No. 5:603–611, 2021

HALLOYSITE NANOTUBE VEHICLES FOR DRUG DELIVERY THROUGH A MODEL BLOOD–BRAIN BARRIER

M. Saleh[1], N. Prajapati[1], A. Karan[1], N. Rahman[1], A. Stavitskaya[2], M. DeCoster[1], and Y. Lvov[1]*

[1]Institute for Micromanufacturing and Biomedical Engineering Program, Louisiana Tech University, Ruston, LA 71270, USA
[2]Gubkin Russian State University, Moscow 119991, Russia

Abstract—Epilepsy treatment requires anti-seizure medical formulations; available medications have various painful side effects and penetrate the brain–blood barrier poorly. A promising method is the use of natural clay nanocontainers for drug delivery through this membrane barrier. Halloysites (Hly) are biocompatible, 50-nm diameter tubes with a positively charged, hollow inner lumen and negatively charged outer shell and are available naturally. These characteristics enable them to be versatile as drug loaded 'nano-torpedoes' effectively penetrating cell membranes. The endothelial cells are a major cell type in the blood–brain barrier that provides for the selective permeability separating the circulating blood and allowing only the passage of glucose, water, and amino acids, but not traditional drug formulations. Nanotubes encapsulating rhodamine isothiocyanate and ionomycin penetration through the rat-brain microvascular endothelial cells followed by a prolonged 24-h drug release was demonstrated. A model membrane was set up across 0.4-μm-pore polystyrene transwell supports covered by seeding endothelial and astrocyte cells to mimic the blood–brain barrier in vivo. This barrier demonstrated a dual permeation mechanism (inter-cell accumulation and through-passing) for loaded Hlys, exploiting the potential of this nanoclay in the trans-membrane delivery of drugs. Use of Hly nanotubes as drug carriers to penetrate the brain microvascular endothelial barrier and to deliver the payload displayed a new approach for the treatment of brain diseases such as epilepsy.

Keywords—Blood–brain barrier · Drug delivery · Halloysite · Nano-torpedo

INTRODUCTION

Roughly one in six people suffers from various types of neurological disorders across the world, and up to 7 million premature deaths occur each year. Brain diseases affect people's way of life negatively through seizures which cause irregular behaviors. Millions of people suffer from epilepsy, making it one of the most common types of brain disorders. The current treatment of epilepsy is poor due to the lack of availability of anti-seizure medication and its lack of effectiveness. Current medication has various side effects such as dizziness and difficulties with speech. Utilizing nanotechnological formulations to treat the disorders could lead to a cure for up to 70% of diagnosed patients (Silva, 2008; Bennewitz & Saltzman, 2009; Bozdağ Pehlivan, 2013; World Health Organization [WHO], 2020). Dopamine and gamma-amino-n-butyric acid are brain neurotransmitters that are important when researching brain disorders such as epilepsy; ionomycin allows the calcium response in brain membrane cells to be followed. In the barrier, brain microvascular endothelial cells are the main layer component making a membrane with blood vessels. Endothelial cells account for much of the proteins that deny access to the brain by pathogens and other toxic substances. This barrier also prevents most anti-seizure medications from reaching the brain tissue (Mahringet al., 2013; Lvov et al., 2016). Using Hly clay nanotubes helps to penetrate the endothelial cells through a 'nano torpedo' approach and effectively delivers the loaded substances over an extended time.

Use of nanotubes that are 50 nm in diameter is effective at penetrating cell membranes due to the small cross-section. In the present case, the tubule penetrability of the materials is defined by their diameters being tens of nanometers rather than by their length – up to a micrometer. This idea allowed introduction of the term 'nano-torpedo' drug delivery; it assumes that the most efficient barrier breaking is achieved by close to perpendicular intrusion of the Hly tubes. Halloysite nanotubes are formed by 10–15 revolutions of 0.72 nm-thick aluminosilicate sheets and have diameters ranging between 40 and 60 nm, lumen diameters of 12–15 nm, and are between 500 and 900 nm long (Fig. 1) (Liu et al., 2014; Lvov et al., 2016). Halloysite is a natural and cheap nanomaterial, available in large quantities. The outer surfaces of Hly are composed of SiO_2, and the interiors are composed of Al_2O_3, which are oppositely (negative/positive) charged in the pH range of 3–9 (Lazzara et al., 2018). The loaded Hly usually has enhanced electrical zeta-potential of –40 to –50 mV allowing for stable aqueous colloids, which is important for the formulated drug injection. The structure of Hly displays how the neurotransmitter can be loaded inside the lumen, which is effective for the adsorption of negatively charged drug molecules. Based on geometrical sizes of Hly, one may conclude that the maximal volume load inside the tubes is 10–12 vol.%, which may reach 15–20 wt.% with adsorption of an external drug (especially a cationic one). This is a typical drug load, as summarized by Santos et al. (2019). Greater drug loading means that drug molecules are adsorbed on the tube external surface, which

This paper belongs to a special issue on 'Clay Minerals in Health Applications'

* E-mail address of corresponding author: ylvov@latech.edu
DOI: 10.1007/s42860-021-00161-6

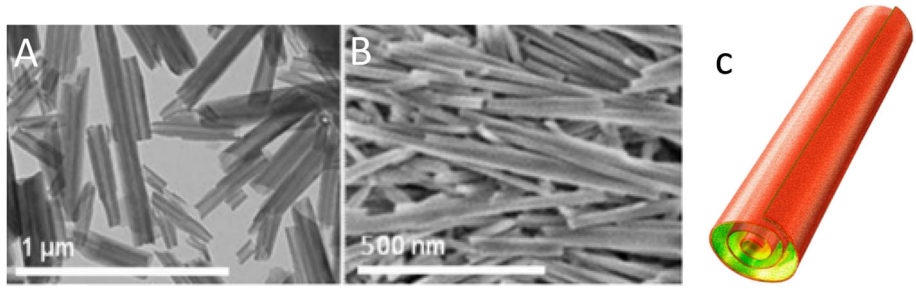

Fig. 1. a TEM and **b** SEM images of Hly, and **c** a schematic image of a rolled clay tube

may change the formulation properties that are observed through zeta-potential and colloidal stability. Thus, inner adsorption of negative molecules usually increases the electrical potential magnitude from ~−30 mV in pristine to –45 to –50 mV in loaded nanotubes (Liu et al., 2014. Drugs such as khellin, oxytetracycline, gentamicin, ciprofloxacin, vancomycin, atorvastatin, metronidazole, dexamethasone, doxorubicin, furosemide, nifedipine, curcumin, resveratrol, povidone, iodine, amoxicillin, brilliant green, chlorhexidine, and DNA and viral genes were loaded successfully in Hly (Santos et al., 2019).

Halloysite is a biocompatible material with low-toxicity assessments (Dzamukova et al., 2015b; Fakhrullina et al., 2019; Hu et al., 2017; Kamalieva et al., 2018; Kruchkova et al., 2016; Mehdia et al., 2018; Vergaro et al., 2010; Wang et al., 2018; Zhao et al., 2019). Researchers reached a consensus that these clay nanotubes are safe at levels of up to 0.5 mg/mL, which is less toxic than common table salt (Vergaro et al., 2010). This was tested on in vitro and in vivo systems: cell lines, microworms, infusoria, fishes, mice, and rats (Santos et al., 2019). The only minor toxic effect was found with significant oral consumption of Hly when acidic clay decomposed in the stomach and increased Al^{3+} accumulation (Kamalieva et al., 2018). The mice that were fed orally with small nanoclay doses (5 mg/kg of mouse weight, which corresponds to a daily consumption of 3 g of Hly for adult humans for 1 month) showed no oxidative stress or other toxicity signs and even demonstrated greater growth rates. Clay nanotubes loaded with drugs will penetrate cells more efficiently than spherical particles of the same mass (Dzamukova et al., 2015a; Wang et al., 2018). This approach allowed for effective delivery by Hly of doxorubicin and other anticancer drugs (Dzamukova et al., 2015a; Yang et al., 2016; Zhang et al., 2019).

In the current work, the penetration of Hly nanotubes into primary rat endothelial cells (BMVECs), the main cell types which prevent the entry of drugs through the blood–brain barrier, were studied (Prajapati et al., 2021; Prajapati & DeCoster, 2020; Rodrigues et al., 2021; Vivès et al., 2008). In addition, a model was developed showing the interaction of tagged Hly with the endothelial lining by layering the cells on a porous membrane in transwell inserts. This was done using fluorescent rhodamine isothiocyanate dye, where Hly binds on the cell, penetrates the cell interior, concentrates around the nuclei, and may deliver a drug load. The Hly/brilliant green formulations with intracellular delivery allowed the preferable elimination of human lung carcinoma cells (A-549) as compared with hepatoma cells due to different intracellular penetration (Dzamukova et al., 2015a).

The transwell assay is used widely to study the absorption in the intestine of molecules administered orally (Artursson, 1991; Artursson et al., 2001; Hubatsch et al., 2007; Stenberg et al., 2001). The development of an in vivo membrane system to mimic in vitro and analyze the transport of loaded Hly tubes across the model (endothelial and astrocyte cells) blood–brain barrier was challenging. Transwell inserts were utilized with a porous polycarbonate membrane which acts as a chamber where a confluent layer is formed on top of astrocytes. The membrane nanotube permeability and the ability to visualize the multilayered cells were realized through non-inverted confocal microscopy (Fig. 2).

Throughout these experiments, the penetration of Hly nanotubes into rat brain microvasculature was analyzed within and outwith the endothelial cells, which are the primary defenders of the brain tissue. Tagging the nanotubes with fluorescent rhodamine B isothiocyanate (RITC) illustrated the ability of Hly to bind to and penetrate the endothelial cell membrane while delivering the payload. Halloysite nanotube formulations can, therefore, be effective carriers for various drugs and neurotransmitters for treating brain diseases. The development of a model for the blood–brain barrier is illustrated in Fig. 1 which shows how a cell insert is used with a porous membrane, attaching one layer of endothelial cells on top of a layer of astrocytes and displaying how the Hly is binding and passing through the model barrier by tagging them with the RITC dye and ionomycin drug. The hypothesis is that Hly tubes acted as 'nano-torpedoes' penetrating the blood–brain barrier and releasing the drug load in a sustained manner. The layer-by-layer construction of the two-type cell model of the blood–brain barrier on transwell inserts was effective at displaying RITC-loaded Hly binding to and penetrating the cell membranes.

MATERIALS AND METHODS

Halloysite was purchased from Sigma Aldrich, St. Louis, Missouri, USA and used without further purification. Rhodamine B isothiocyanate and ionomycin were also obtained from Sigma Aldrich. For system analysis, scanning and

https://doi.org/10.1007/s42860-021-00161-6 Published online by Cambridge University Press

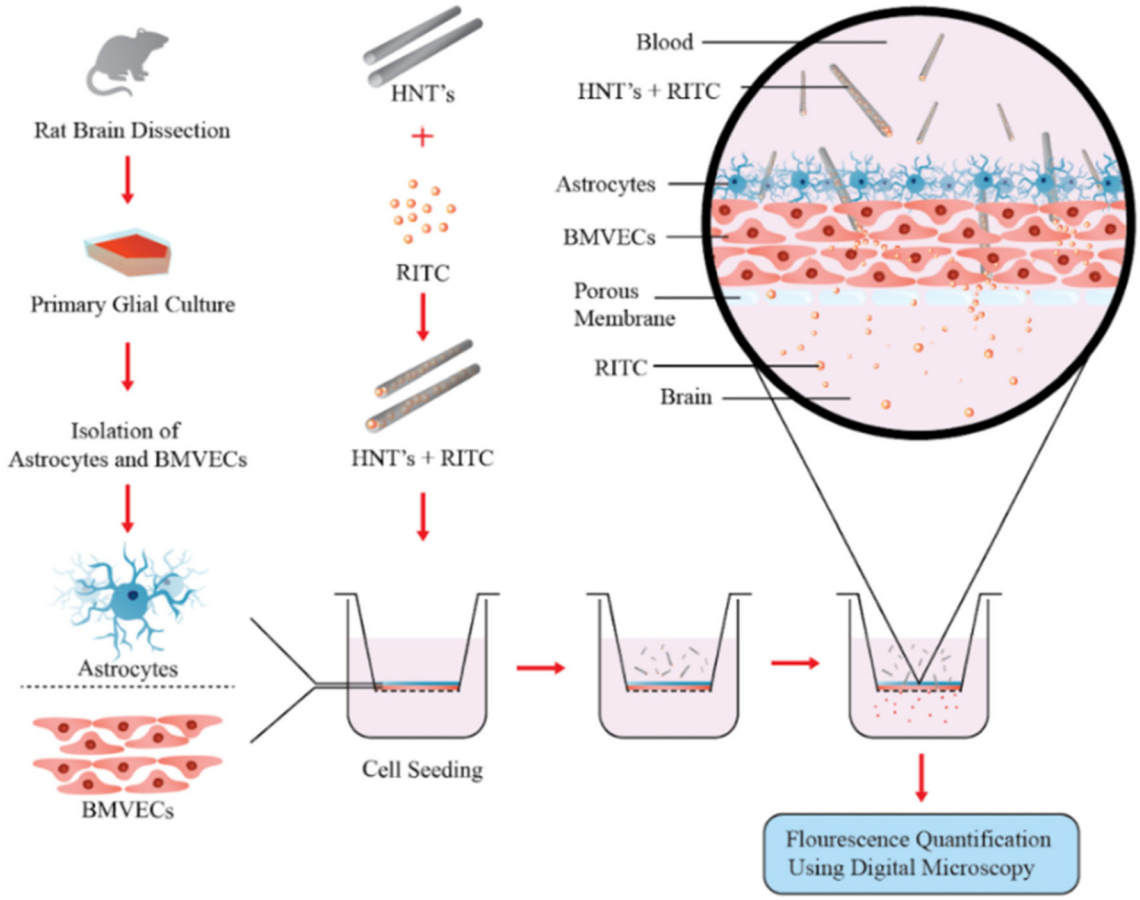

Fig. 2. A co-culture model of brain endothelium and astrocyte membrane developed for testing the penetration and delivery of Hly nanotubes and their payload (RITC) across the blood–brain barrier model

transmission electron microscopes were used (EDAX-SEM, Hitachi-S4800,Tokyo, Japan, and TEM, JEM-2100, JEOL, Tokyo, Japan) as well as thermogravimetric analysis (TGA, Thermal Advantage Q50, New Castle, Delaware. USA), UV-Vis spectrophotometry (Agilent 8453, Santa Clara, California, USA), fluorescent and laser confocal optical microscopy (Leica DMI 6000 B inverted microscope and Nikon A1R Confocal and Super Resolution System, Allendale, New Jersey, USA). A ZetaPlus Instrument (Brookhaven Instruments, Holtsville, New York, USA) was used to determine the system's surface charge.

Harvesting of Primary Endothelial Cells – BMVECs and Astrocytes

Sprague Dawley rat pups were euthanized by cervical disarticulation between post-natal days 1 and 3. All procedures were performed by adhering to the protocol approved by the Institutional Animal Care and Use Committee, Louisiana Tech, USA. Cells were isolated from the cortex of the rat pups and cultured in F12 Nutrient Mixture consisting of 10% horse serum and 10% fetal bovine serum (FBS), as described previously. The primary glial cells thus obtained were treated with 5.51 μM of puromycin (Sigma Aldrich) and cultured in rat endothelial growth medium (Cell Applications Inc., San Diego, CA, USA), containing 6% rat endothelial growth factor, to obtain pure endothelial (BMVECs) culture (Bennewitz & Saltzman, 2009; Bozdağ Pehlivan, 2013). The astrocytes were purified by subculturing the glial cells in Ham's F-12K medium with 5% FBS and 5% horse serum and washing off the overlaying microglial cells regularly before subculturing. The purity of each culture was determined by staining the cells against their specific markers, glial fibrillary staining against astrocytes, and Von Willebrand factor staining against endothelial cells (Mahringer et al., 2013).

Binding Hly with RITC Dye

The samples which contained Hly nanotubes (Hly) were developed by tagging RITC and loading ionomycin through mixing, centrifugation, and sonication (Eppendorf Centrifuge and Sonicator, Westbury, New York, USA) at various ratios and speeds, including 10 mg Hly/mL of DI water and a 2:1 ratio of RITC. The solutions were then sonicated for 1 min and put on a stir plate for 24 h at room temperature. The mixture was washed once through centrifugation at 700×*g* for 2.5 min and then vacuumed and dried at 70°C for 24 h. When using ionomycin, 20 mg of Hly tubes were loaded with the

https://doi.org/10.1007/s42860-021-00161-6 Published online by Cambridge University Press

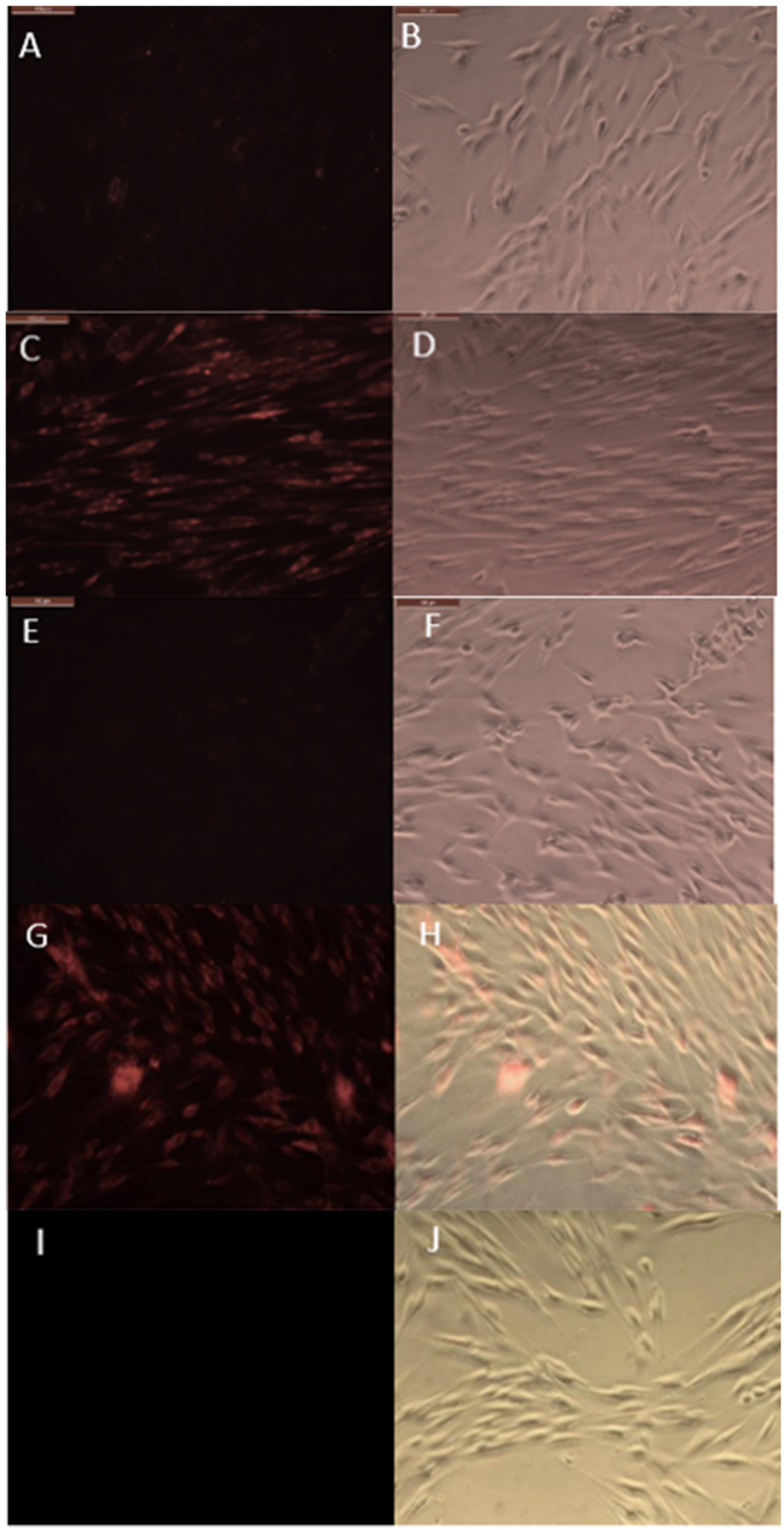

Fig. 3. Endothelial cells-BMVEC treated with Hly loaded with RITC after displaying fluorescence and direct images in time frames of: **a**, **b** and **e**, **f** 4 h; **c**, **d** and **g**, **h** 24 h phase, magnification. Positive controls; BMVECs treated with non-encapsulated rhodamine after 4 h: **e**,**f** fluorescence and direct images; **g**, **h** the same after a 24 h phase. **i**,**j** images are negative controls with unlabeled Hly. Direct phase and fluorescence microscopic imaging of primary endothelial cells that were treated with Hly only. Scale bars: 100 μm

https://doi.org/10.1007/s42860-021-00161-6 Published online by Cambridge University Press

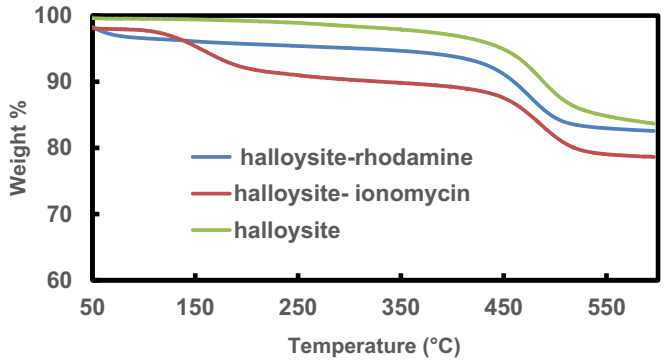

Fig. 4. Thermogravimetric curves of pristine Hly, Hly loaded with rhodamine, and Hly loaded with ionomycin.

ionophore and mixed with 1 mM ionomycin for 24 h. The formulation was then cleaned with DI water by centrifugation at 700×*g* for 3 min. The solution was freeze-dried for 20 min and placed in a vacuum for 24 h to remove excess solution. The sample characterizations were obtained by a zeta potential analyzer (TA Instruments Zeta Potential Analyzer, Holtsville, New York, USA), which displays the surface charge and thermogravimetric analysis, to calculate the loading percentage.

Rhodamine Isothiocyanate Release Profile

Using 10 mL of endothelial media, 3.3 mg of Hly-rhodamine was taken and stirred at 250 rpm for 24 h. Readings were taken after 1, 4, 8, and 24 h.

Visualization of Hly-RITC Uptake and Diffusion Across the Barrier

A concentration of 20 μg/mL of Hly-RITC formulation was added to the cell inserts without cells (media alone), to cell inserts with a monolayer of endothelial cells, and to inserts with a bilayer of endothelial and astrocyte cells developed on the porous membrane. The concentration was tested in two separate passages of cells in triplicated wells. Hly-RITC formulations were added on top of the cell bilayer. Images of the solution beneath the cell culture inserts were taken using a Leica DMI 6000 B inverted microscope (LEICA Leica DMI 600 B, Allendale, New Jersey, USA) at intervals of 4 and 24 h, after the addition of the material. The images were checked for penetration of the nanotubes and fluorescence intensity due to diffusion of RITC from Hly across the membrane to the solution in bottom wells. The fluorescence intensity for the images at the two time points was quantified using *MATLAB* to compare the diffusion across the barrier with the control wells (inserts) without cells.

Development of the in vitro Co-culture Model on Transmembrane

Astrocytes were plated at a density of 20,000 cells per well onto the cell-culture inserts (Thermo Fisher Scientific) with a porous polycarbonate (PC) membrane of 0.4-μm pore diameter, and grown at 37°C in 5% CO_2 in humidified incubators. At 50–70% confluency, endothelial BMVEC cells were seeded on top of the astrocytes at 20,000 cells per well to ensure the bilayer organization. The development of a confluent bilayer of endothelial and astrocyte cells was determined by using confocal microscopy.

MTT Assay

An MTT (3-(4,5-dimethylthiazol-2-yl)-2,5-diphenyl tetrazoloim bromide) assay was performed to compute cell metabolism as a measure of cytotoxicity, as described previously (Vivès et al., 1997). Cells were cultured in 48-well

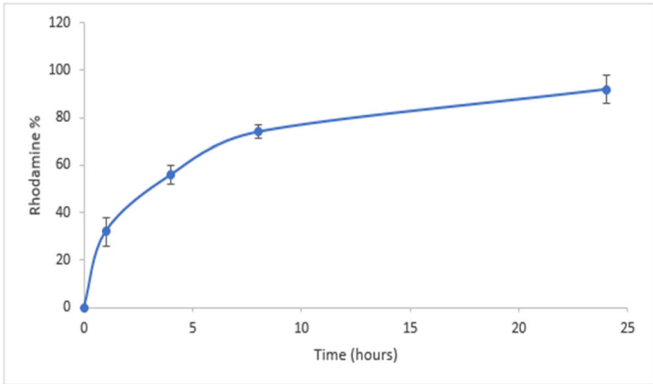

Fig. 5. Release profile of rhodamine isothiocyanate-RITC loaded into Hly taken at 555 nm

https://doi.org/10.1007/s42860-021-00161-6 Published online by Cambridge University Press

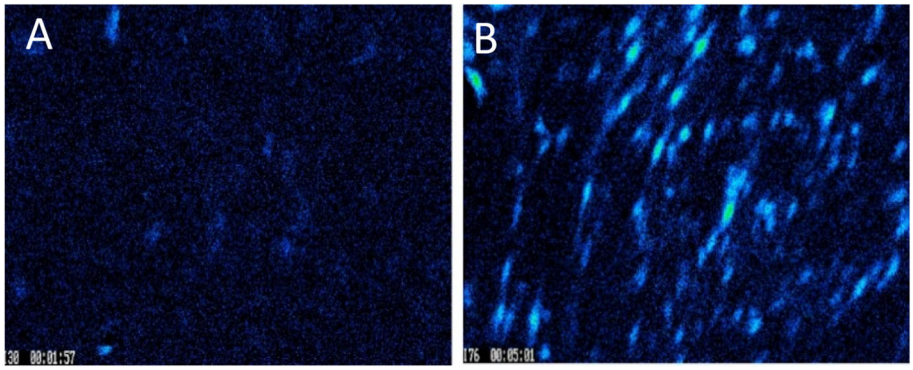

Fig. 6. Images captured for endothelial cells-BMVECs during Ca^{2+} treatment: **a** peak stimulation by 50 μg/mL of empty Hly nanotube, and **b** peak stimulation by 50 μg/mL nanotubes loaded with ionomycin.

culture plates (Griener, Vienna, Austria) at 37°C and 5% CO_2 in humidified incubators. The cells were then treated with various concentrations of Hly-RITC when their y confluency reached 60–70%. The control wells received media with no materials. After 24 h of treatment, MTT (1.25 mg/mL in RPMI media) was added to the cells and incubated for 1 h at 37°C. The absorbance of the resulting formazan crystals dissolved in 90% isopropyl alcohol was read at 570 nm. Cytotoxicity was computed by comparing the absorbance of Hly-RITC-treated wells with the control wells.

Statistical Analysis

Statistical comparison for diffusion through the barrier was performed using one-way ANOVA with the multiple comparison method for experiments consisting of more than two groups and two-tailed t-tests for comparison between two groups. The results were considered statistically significant when $p < 0.05$. Values are presented as the mean ± standard error of the mean of $n = 6$ wells for each experiment.

RESULTS AND DISCUSSION

Intracellular Rhodamine Isothiocyanate Delivery with Hly Nanotubes

Halloysite nanotubes are very capable of encapsulating, transporting, and slowly releasing the dye or drugs. Note that the surface of the Hly was not modifiedwith any type of polymer or silane coating. The penetration of the fluorescent RITC-loaded Hly into the layer of endothelial cells is shown in Fig. 3. The timeframe of the images is 4 and 24 h after release of the payload, for Hly + RITC and 2 μg/mL of RITC alone. The loading formulation of RITC in Hly was 20 wt.%, thus making the same amount added to the samples. The small bright dots found in the images of Fig. 3c are the aggregated Hly tubes that contain RITC. After 4 h, Hly-RITC aggregations were displayed mostly along the cellular membrane and inside the endothelial cells; those are indicated by nuclear exclusion. An image of only RITC added, and at the same concentration, is given in Fig. 3e–f, displaying a much dimmer visualization of the cell's interaction with this non-encapsulated dye.

Results for the 24 h treatment were similar with brighter fluorescence in both conditions but RITC-loaded Hly delivered more dye into the cells compared to the dye alone (Fig. 3). Images taken after 24 h displayed the nanotube distribution more evenly over the cell interior and within the cell body. The RITC-Hly was seen to be concentrated in smaller spots of ~1 μm, which may be the nuclear surroundings, as was found for MCF-7 cells treated with Hly (Vergaro et al., 2010). Throughout the experiments, detection of nuclear exclusion through the use of fluoresence displayed cells, indicating that the nanotubes did not stress or kill the cells. The nanoclays appear as small dots in Fig. 3c and are brighter than the non-encapsulated dye spread inside the cells. Displaying localized nanotubes with red dye in the cell cytoplasm with a distinct nuclear exclusion shows a greater binding. Hly-RITC cells showed significant fluorescence, indicating a prolonged delivery of the dye from the nanotubes.The cells treated with Hly nanotubes

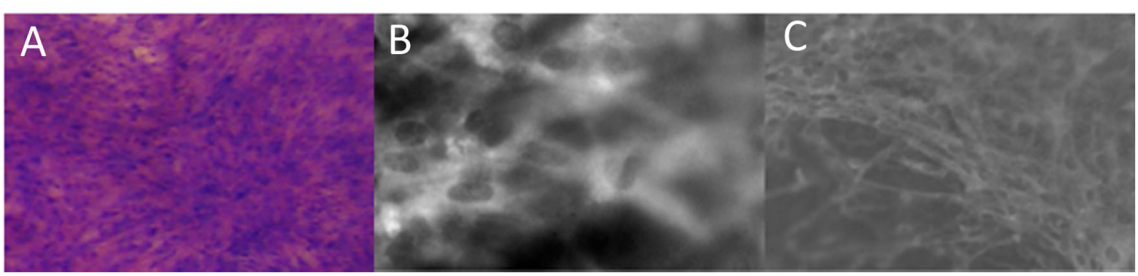

Fig. 7. DiffQuik-stained images of a model brain barrier of **a**co-cultured endothelial astrocytes plated on a porous membrane. **b**, **c** (z-stack images with a 0.3 μm step size) of non-inverted microscopy images of the transwell assay with a layer of **b** astrocytes and **c** endothelial cells

https://doi.org/10.1007/s42860-021-00161-6 Published online by Cambridge University Press

Fig. 8. Controls **a**20μg/mL HLy-RITC fluorescence intensity **(**no cell inserts, direct addition to the bottom well), **b**20μg/mL HLy-RITC added to the support, and **c** membrane support treated with media alone

alone (negative controls) showed no fluorescence (Fig. 3c,d and g,h).

Thermogravimetric Analysis, TGA

Thermogravimetric analysis was used to determine the sample's weight change during the component burning (Fig. 4) and demonstrated that the material or substance was loaded inside the nanotubes and gave an approximate percentage of the amount loaded. The TGA analysis (Thermal Advantage Q50, New Castle, Delaware, USA) was done using pristine Hly with a major phase transition at 490°C, with some nanotubes loaded with RITC, and others loaded with ionomycin. The difference in mass decrease during heating between pristine and loaded Hly (Fig. 4a–c) gave an estimated RITC loading of 5 ± 1 wt.%. A similar analysis for ionomycin drug loading into the nanotubes gave values of 14 ± 1 wt.%, indicating some external drug attachment. The results showed that, compared to pristine Hly, an ionomycin loading of ~8 wt.% was achieved.

Hly Loaded Release Profile

The loaded Hly samples that were used to treat the endothelial cells were tested for RITC release kinetics (Fig. 5). This displays the rate at which the dye is released over a period of 24 h. The results showed that rhodamine is released in an initial burst of ~25% within the first 1 h, which is an expected characteristic when utilizing Hly nanocontainers. This caused no stress to the endothelial cells. During a further period, the advantages of Hly tubes began to become apparent, i.e. by releasing the dye slowly over a period of 24 h at a steady rate (releasing the remaining 75% over the next 23 h). The delivery process avoids major spikes that could stress or kill the cells. The nanotubes penetrated cell nuclei during the initial 4 h experiment in Fig. 3a,b,e,f. The red dots which represent the loaded Hly were confined within the cells; although they are extremely dim in these pictures, the visualization of drug release begins.

Hly-loaded Ionomycin: Calcium Imaging

A good method to visualize ionomycin-loaded HNT is the calcium response (Saleh et al., 2020). With real-time calcium imaging, the cell's response to ionomycin had a spiked increase in Ca^{2+} which decayed quickly due to clearance by cells. When Hly was used alone, the response was small (Fig. 6a). When ionomycin was loaded inside the tubules, achieving a greater response of Ca^{2+} for the same concentration of 1 μM (the bright blue color represents the cells responding to the ionophore) that was also used resulting in a gradual increase in calcium which remained higher for a greater period of time. This experiment also showed that the introduction of Hly maintained a stable and slow release of drug over 4 h without stressing the cells.

Co-culture Studies of Blood–Brain Barrier

The confluence of the bilayer of astrocyte and endothelial cells was examined using a non-inverted microscope after Diff-Quik staining of the cells (Fig. 7a). When a continuous monolayer was ensured, the additional cells were examined using non-inverted confocal microscopy to indicate the two cells assay (Fig. 8b,c– both astrocyte and endothelial), based on the cell dimensions that have been seen on two distinct planes (0.3 μm step in the *z*-axis). The co-culture model of

Fig. 9. Results of Hly penetration though the membrane: **a**,**b** fluorescent intensity of the solution beneath the co-culture brain–barrier model after 4 and 24 h of treatment. **c** The membrane cell viability after 24 h of treatment with Hly and copper nanomaterials as a negative control

https://doi.org/10.1007/s42860-021-00161-6 Published online by Cambridge University Press

endothelial and astrocyte cells was, thus, produced. This represented a simulated brain barrier microenvironment where these two cell types (endothelial which are brain cells that make up the vascular structure and astrocytes, one of the main structural cells), are present in the complex layer holding the glial cells and neurons together.

Passage of RITC through the Co-culture Model

The fluorescent intensity of the endothelial and astrocyte bilayer as well as images of solution beneath the cell inserts after the treatment with 'nano-torpedo' clay formulations are shown in Fig. 8, part a of which displays the dispersion of RITC-loaded Hly without the cell membrane. The intensity of rhodamine that is released by Hly after passing through the transmembrane for 4 h is shown in Fig. 8b. A negative control where the media alone is present, i.e. no Hly or rhodamine, is shown in Fig. 8c– no fluorescence signal was observed. Understanding the function of the transmembrane which allows the gradual passage of the rhodamine and partial passage of Hly in some cases, was one of the main purposes of the present study.

The treatment conditions were as follows: 20 μg/mL Hly-RITC formulations were placed on top of the well with the designed bi-cell membrane for an analysis of a time-dependent passage of a rhodamine nano-torpedo through the co-culture barrier model membrane over a period of 24 h. The RITC fluorescence intensity under the membrane increased significantly from the 4-h to the 24-h treatment time, indicating penetration by the Hly carrier. The fluorescence signal grew moderately in the first hour but by 24 h it had increased to 85%. Some decrease in the fluorescence intensity at the 4-h time point occurred because the co-culture cell membrane absorbed some of the upcoming rhodamine but further passing enhanced the signal growth beneath the model barrier (Fig. 9a,b). The Hly nanotubes being utilized in drug delivery were probably as efficient as this because of the predominantly vertical penetration through the cell membrane. An MTT assay was performed 24 h after treatment of the cells plated at 10,000 per mL when they reached 60% confluency to assess cell metabolism as the measure of cytotoxicity (Fig. 9c).

The results indicated that the empty Hly nanotubes did not affect the cell metabolism in BMVECs and, hence, showed no significant sign of toxicity as the cellular metabolism was observed to be within 1–2% for the treatment of 10, 25, and 50 μg/mL of Hly, compared to control cells treated with media alone. Positive control of toxicity with 6 μg/mL of copper nanotubes (CuNPs) added demonstrated inhibition of the cell metabolism by 27% within 24 h.

CONCLUSIONS

Hly nanotubes deployed as 'torpedoes' were used to penetrate the brain microvascular endothelial cell membrane and released their ionomycin payload effectively in vitro over an extended time period. This approach showed that Hly interacted with the barrier cells, not only binding them but also penetrating inside to the vicinity of the nuclei without causing any cell toxicity The release of the loaded rhodamine isothiocyanate and ionomycin (3 and 8 wt.%) from the nanotubes was extended for >24 h. The development of a blood–brain barrier model, which consists of a 0.4 μm porous polystyrene transwell support covered by sequential seeding of endothelial and astrocyte cells was realized. Layering of endothelial and astrocyte cells on top of each other created a model of the brain barrier which could be tested for penetration by the nanotubes. The nanotubes were found to have penetrated partially the cell membrane while releasing the drug payload past this barrier. Hly nanotubes capable of passing the model barrier have potential as drug carriers to aid in the fight against brain disease.

ACKNOWLEDGMENTS

Support by NSF – grant 1632891 is acknowledged. Any opinions, findings, and conclusions or recommendations expressed in this report are those of the authors and do not necessarily reflect the view of the National Science Foundation. YL and AS thank the Russian Science Foundation (Grant 19-79-30091). Bishan Pandey and Rawil Fakrulin are thanked for providing Figs 2 and 1c, respectively.

Funding

Funding sources are as stated in the Acknowledgments.

Compliance with ethical statements

Conflict of Interest

The authors declare that they have no conflict of interest.

REFERENCES

Artursson, P. (1991). Cell cultures as models for drug absorption across the intestinal mucosa. *Critical Reviews in Therapeutic Drug Carrier Systems, 8*(*4*), 305–330.

Artursson, P., Palm, K., & Luthman, K. (2001). Caco-2 monolayers in experimental and theoretical predictions of drug transport. *Advanced Drug Delivery Reviews*, *46(1–3),* 27–43. 10.1016/S0169-409X(00)00128-9 (The article was published originally in *Advanced Drug Delivery Reviews*, *22*, (1996), 67–84.)

Bennewitz, M. F., & Saltzman, W. M. (2009). Nanotechnology for delivery of drugs to the brain for epilepsy. *Neurotherapeutics, 6*(*2*), 323–336. https://doi.org/10.1016/j.nurt.2009.01.018

Bozdağ Pehlivan, S. (2013). Nanotechnology-based drug delivery systems for targeting imaging and diagnosis of neurodegenerative diseases. *Pharmaceutical Research, 30*(*10*), 2499–2511. https://doi.org/10.1007/s11095-013-1156-7

Dzamukova, M., Naumenko, E., Badrutdinov, A., Lvov, Y., & Fakhrullin, R. (2015a). Enzyme-activated intracellular drug delivery with tubule clay nanoformulation. *Scientific Reports, 5*, *10560*. https://doi.org/10.1038/srep10560

Dzamukova, M., Naumenko, E., Rozhina, E., Trifonov, A., & Fakhrullin, R. (2015b). Cell surface engineering with polyelectrolyte-stabilized magnetic nanoparticles: A facile approach for fabrication of artificial multicellular tissue-mimicking clusters. *Nano Research, 8*, 2515–2532. https://doi.org/10.1007/s12274-015-0759-1

Fakhrullina, G., Khakimova, E., Akhatova, F., Lazzara, G., Parisi, F., & Fakhrullin, R. (2019). Selective antimicrobial effects of curcumin @ halloysite nanoformulation: A *Caenorhabditis elegans* study.

https://doi.org/10.1007/s42860-021-00161-6 Published online by Cambridge University Press

ACS Applied Materials and Interfaces, 11, *23050–23064*. https://doi.org/10.1021/acsami.9b07499

Hu, Y., Chen, J., Li, X., Sun, Y., Huang, S., Li, Y., Liu, H., Xu, J., & Zhong, S. (2017). Multifunctional halloysite nanotubes for targeted delivery and controlled release of doxorubicin in-vitro and in-vivo studies viability tests and microscopy study. *Nanotechnology, 28*, *375101*. https://doi.org/10.1088/1361-6528/aa8393

Hubatsch, I., Ragnarsson, E., & Artursson, P. (2007). Determination of drug permeability and prediction of drug absorption in Caco-2 monolayers. *Nature Protocols, 2*, 2111–2119. https://doi.org/10.1038/nprot.2007.303

Kamalieva, R., Ishmukhametov, I., Batasheva, S., Rozhina, E., & Fakhrullin, R. (2018). Uptake of halloysite clay nanotubes by human cells: Colourimetric. *Nano Structure Nano Objects, 15*, 54–60. https://doi.org/10.1016/j.nanoso.2018.03.009

Kruchkova, M., Danilushkina, A., Lvov, Y., & Fakhrullin, R. (2016). In vivo toxicity study of nanoclays and graphene oxide with Paramecium caudatum. *Environmental Science: Nano, 3*, 442–452. https://doi.org/10.1039/c5en00201j

Lazzara, G., Cavallaro, G., Panchal, A., Fakhrullin, R., Stavitskaya, A., Vinokurov, V., & Lvov, Y. (2018). An assembly of organic-inorganic composites using halloysite clay nanotubes. *Current Opinion in Colloid & Interface Science, 35*, 42–50. https://doi.org/10.1016/j.cocis.2018.01.002

Liu, M., Jia, Z., Jia, D., & Zhou, C. (2014). Recent advance in research on halloysite nanotubes-polymer nanocomposite. *Progress in Polymer Science, 39*(*8*), 1498–1525. https://doi.org/10.1016/j.progpolymsci.2014.04.004

Lvov, Y., Wang, W., Zhang, L., & Fakhrullin, R. (2016). Halloysite clay nanotubes for loading and sustained release of functional compounds. *Advanced Materials, 28*(*6*), 1227–1250. https://doi.org/10.1002/adma.201502341

Mahringer, A., Ott, M., & Fricker, G. (2013). The blood–brain barrier: An introduction to its structure and function. The Blood–Brain Barrier, pp. *1–20*. Springer, Berlin, https://doi.org/10.1007/7355_2013_20

Mehdia, Y., Fizira, M., Itatahinea, A., Hea, H., & Dramoua, P. (2018). Preparation of multifunctional PEG-graft-halloysite nanotubes for controlled drug release, Tumor cell targeting, and bio-imaging. *Colloidal Surfaces B Biointerface., 170*, 322–329. https://doi.org/10.1016/j.colsurfb.2018.06.042

Prajapati, N., & DeCoster, M. (2020). Nitric oxide modulation and calcium dysregulation in brain endothelial and astrocyte cell co-cultures during inflammation. *Biomedical Sciences Instrumentation, 56*, 24–27.

Prajapati, N., Karan, A., Khezerlou, E., & DeCoster, M. A. (2021). The immunomodulatory potential of copper and silver based self-assembled metal organic biohybrids nanomaterials in cancer theranostics. *Frontiers in Chemistry, 8*, 1296. https://doi.org/10.3389/fchem.2020.629835

Rodrigues, J. P., Prajapati, N., DeCoster, M. A., Poh, S., & Murray, T. A. (2021). Efficient LRP1-mediated uptake and low cytotoxicity of peptide L57 in vitro shows its promise as CNS drug delivery vector. *Journal of Pharmaceutical Sciences, 110*(2), 824–832. https://doi.org/10.1016/j.xphs.2020.09.019

Saleh, M. Y., Prajapati, N., DeCoster, M. A., & Lvov, Y. (2020). Tagged halloysite nanotubes as a carrier for intercellular delivery in brain microvascular endothelium. *Frontiers in Bioengineering and Biotechnology, 8*, 451. https://doi.org/10.3389/fbioe.2020.00451

Santos, A. C., Pereira, I., Reis, S., Veiga, F., Saleh, M., & Lvov, Y. (2019). Biomedical potential of clay nanotube formulations and their toxicity assessment. *Expert Opinion on Drug Delivery, 16*(*11*), 1169–1182. https://doi.org/10.1080/17425247.2019.1665020

Silva, G. A. (2008). Nanotechnology approaches to crossing the blood-brain barrier and drug delivery to the CNS. *BMC Neuroscience, 9*(Suppl 3), S4. https://doi.org/10.1186/1471-2202-9-S3-S4

Stenberg, P., Norinder, U., Luthman, K., & Artursson, P. (2001). Experimental and computational screening models for the prediction of intestinal drug absorption. *Journal of Medicinal Chemistry, 44*(*12*), 1927–1937. https://doi.org/10.1021/jm001101a

Vergaro, V., Abdullayev, E., Lvov, Y. M., Zeitoun, A., Cingolani, R., Rinaldi, R., & Leporatti, S. (2010). Cytocompatibility and uptake of halloysite clay nanotubes. *Biomacromolecules, 11*(3), 820–826. https://doi.org/10.1021/bm9014446

Vivès, E., Brodin, P., & Lebleu, B. (1997). A truncated HIV-1 tat protein basic domain rapidly translocates through the plasma membrane and accumulates in the cell nucleus. *Journal of Biological Chemistry, 272*(25), 16010–16017. https://doi.org/10.1074/jbc.272.25.16010

Vivès, E., Schmidt, J., & Pèlegrin, A. (2008). Cell-penetrating and cell-targeting peptides in drug delivery. *Biochimica et Biophysica Acta (BBA) - Reviews on Cancer, 1786*(2), 126–138. https://doi.org/10.1016/j.bbcan.2008.03.001

Wang, X., Gong, J., Gui, Z., Hu, T., & Xu, X. (2018). Halloysite nanotubes-induced Al accumulation and oxidative damage in liver of mice after 30-day repeated oral administration. *Environmental Toxicology, 33*(6), 623–630. https://doi.org/10.1002/tox.22543

World Health Organization. (2020). Epilepsy. www.who.int/news-room/fact-sheets/detail/epilepsy. Accessed July 2021

Yang, J., Wu, Y., Shen, Y., Zhou, C., Li, Y.-F., He, R.-R., & Liu, M. (2016). Enhanced therapeutic efficacy of doxorubicin for breast cancer using chitosan oligosaccharide-modified halloysite nanotubes. *ACS Applied Materials and Interfaces, 8*, 26578–26590. https://doi.org/10.1021/acsami.6b09074

Zhang, Z., Luo, X., Wu, Y.-P., Wu, F., Li, Y.-F., He, R.-R., & Liu, M. (2019). Rod in tube: A novel nanoplatform for highly effective chemo-photothermal combination therapy toward breast cancer. *ACS Applied Materials and Interfaces, 11*, 3690–3703. https://doi.org/10.1021/acsami.8b17533

Zhao, X., Wan, Q., Fu, X., Meng, X., Ou, X., Zhong, R., Zhou, Q., & Liu, M. (2019). Toxicity evaluation of one-dimensional nanoparticles using *Caenorhabditis elegans*: a comparative study of halloysite nanotubes and chitin nanocrystals. *ACS Sustained Chemical Engineering, 7*, 18965–18975.

(Accepted: 29 September 2021)